Proceedings of the 28th IEEE
EMBS Annual International Conference
New York City, USA, Aug 30-Sept 3, 2006

A model selection approach for robust spatio-temporal analysis of dynamics in 4D fluorescence videomicroscopy

Ikhlef Bechar and Alain Trubuil

***Abstract*— We describe a novel automatic approach for vesicle trafficking analysis in 3D+T videomicroscopy. Tracking individually objects in time in 3D+T videomicroscopy is known to be a very tedious job and leads generally to unreliable results. So instead, our method proceeds by first identifying trafficking regions in the 3D volume and next analysing at them the vesicle trafficking. The latter is viewed as significant change in the fluorescence of a region in the image. We embed the problem in a model selection framework and we resolve it using dynamic programming. We applied the proposed approach to analyse the vesicle dynamics related to the trafficking of the RAB6A protein between the Golgi apparatus and ER cell compartments.**

I. Introduction

With the advent of new live-cell imaging modalities (wide field videomicroscopy, confocal videomicroscopy, FRAP, FLIM, etc…) made possible by the development in marker technology (GFP) (Chalfie *et al.* 1994)) and fluorescence microscopes, it has become possible to collect *in vivo* vast amounts of spatio-temporal image data. Hence, there is an increasing need for providing automatic tools for the analysis of such image data (see *eg.* [10] for the motivation behind dynamic bioimaging). So far, many techniques inspired from classical video processing have been applied more or less successfully to videomicroscopy processing: Operational research techniques (Danuser et *al.*, 2003); IMM filter tracking (Olivo Marin et *al.*, 2004)); optical flow (Miura et *al.*, 2005); minimal paths in the spatio-temporal domain (Cohen et *al.*, 2005); kymograms (Sibarita et *al.*, 2006).

However, due to the low SNR of videomicroscopic data (Kervrann *et al.*, 2005), the density of objects in the scene, the complexity of their dynamics, the dynamic nature of the background (Kervrann *et al.*, 2006), etc…, other techniques taking into account all these aspects are expected. In this paper, we claim a different approach from the aforementioned ones as no individual tracking of the objects in the scene is needed to analyse the vesicle dynamics. Indeed, our approach proceeds by first detecting activity regions of the sequence. Next, we use an original bidimensional signal processing technique to analyse locally the fluorescence of the pixels of each detected activity region. Finally, trafficking is detected as significant change in the fluorescence of some or whole pixels of a given activity region. Using this analysis, many local and global statistitcs decribing vesicle dynamics can then be computed acoordingly. We used the developed approach to summmarize and analyse the vesicle dynamics related to the trafficking of the RAB6A protein between the Golgi apparatus and ER cell compartments.

* This work was supported by the French Ministery of Resarch - Project IMBIO-MODYNCELL5D:http://www.irisa.fr/vista//ftp/ckervran/ACI-IMPBIO/MODYNCELL5D.html

I. Bechar is a PHD student at University René Descartes (Paris 5), Paris, France, and prepares his PHD in the laboratory of Applied Mathematics and Computer Science, INRA, Domaine de Vilvert, 78352 Jouy-en-Josas, France, and in the laboratory of MAP5, 45 rue des Saints-Pères, 75270 Paris cedex 06, France. ikhlef.bechar@jouy.inra.fr

Dr. A. Trubuil is the Head of the laboratory of Applied Mathematiques and Computer Science, INRA, 78352 Jouy-en-Josas, France. alain.trubuil@jouy.inra.fr

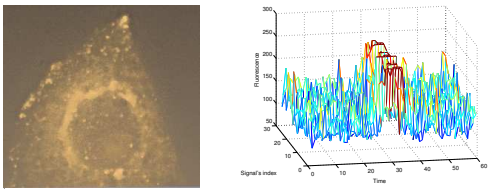

(a) (b)

Fig. 1. *(a) A volume rendering of a 3D videomicroscopic image ; (b) A packet of 27 neighbouring signals. The figure shows a significant change in the fluorescence of some of the 27 pixels between instants* 30 *and* 40 *due to vesicle passage (Colour is for visualization convenience only).*

II. Method description

A. The basic idea of the method

Our key idea for analysing the vesicle trafficking in 3D+T videomicroscopic sequences is that a highly constrasted object, when crossing a given pixel of the 3D scene, makes the fluorescence of this pixel passing from a low to a higher value(*cf.* Fig1.b) during a few time instants. This enables the dynamics of the scene to be described by the sojourn times of objects at the different sites (regions) of the scene. To achieve robustness, instead of individual signals[1], packets of neighbouring signals are used for the analysis.

B. A Model selection framework for spatio-temporal analysis of videomicroscopic data

Consider a group of M unidimensional signals $y_i, i = 1, \ldots, M$. We suppose that each signal $y_i, i = 1, \ldots, M$ can be decomposed as the sum of a deterministic part S (expectation value) and a random part ϵ modeled as white Gaussian noise with standard deviation σ:

$$y_i(t) = S_i(t) + \epsilon_i(t), \quad i = 1, \ldots, M, \quad t = 1, \ldots, N \quad (1)$$

The question we will try to answer through this section is how one can estimate S only from data.

[1]We mean by a signal the temporal profile of the fluorescence of a pixel.

1) Designing models and building estimators for S: In the light of the ideas we presented in section II, an *ideal* model for S captures all simultaneous jumps in the intensity of any sub-group of the M signals $y_i, i = 1, \ldots, M$ and estimates exactly the corresponding intensity levels. Then a model for S spans the space $\mathcal{M}$ of the piecewise constant functions defined in the spatio-temporal domain. So, consider a partition of the interval of time $[1, N]$ which we denote by $\mathcal{T}$. To each time interval $\tau \in \mathcal{T}$, we associate a partition of signal indexes $\mathcal{I}_\tau$. Then a model for S is given by:

$$S_i(t) = \sum_{k=1}^{|\mathcal{T}|} \sum_{j=1}^{|\mathcal{I}_k|} S_{k,j} \mathbb{1}_{\mathcal{I}_{k,j}}(i) \mathbb{1}_{\mathcal{T}_k}(t) \quad (2)$$

We assume that $|\mathcal{I}_k| \leq p$. Though our approach can work for an arbitrary p, herein, we consider only the case where $p = 2$ (a pixel either belongs to an object or to the background).

Now, let's construct estimators of S from data. For this, suppose we are given a spatio-temporal partition $m = \{I_{k,j}, 1 \leq k \leq |\mathcal{T}|, 1 \leq j \leq |\mathcal{I}_k|\}$, and we want to build an estimator $\hat{S}_m$ for S accordingly. If one chooses the $\mathcal{L}^2$ distance as a metric for assessing the quality of $\hat{S}_m$, then:

$$\hat{S}_m = \sum_{k=1}^{|\mathcal{T}|} \sum_{j=1}^{|\mathcal{I}_k|} \overline{S}_{k,j} \mathbb{1}_{\mathcal{I}_{k,j}}(i) \mathbb{1}_{\mathcal{T}_k}(t),$$

$$\text{where} \quad \overline{S}_{k,j} = \frac{1}{|\mathcal{I}_{k,j}|} \sum_{t \in \mathcal{T}_k} \sum_{i \in I_{k,j}} y_i(t)$$

The dimension of an estimator $\hat{S}_m$ is defined as $D_m = |m|$.

2) A penalized criteria for the estimation of S - Theoretical background: Let $\mathcal{M}$ be a family of models to which we associate a family $\mathscr{S} = \{\hat{S}_m, m \in \mathcal{M}\}$ of estimators of S. We seek for the estimator $\hat{S}_m \in \mathscr{S}$ which minimizes the quadratic risk $\mathbb{E}\|S - \hat{S}_m\|^2$. As $\mathbb{E}\|S - \hat{S}_m\|^2$ cannot be minimized directly from data[1][9], a sharp upper bound of this risk is minimized using data. A known approach in model selection literature is the penalized least squares criteria where one minimizes a criteria of the form:

$$crit(\hat{S}_m) = \gamma(\hat{S}_m) + \text{pen}(m) \quad (3)$$

where $\gamma(\cdot)$ stands for the $\mathcal{L}^2$ distance to the data y, and pen$(\cdot)$ stands for a penalty on the model's complexity. The Mollows' *CP*, AIC and BIC are examples of such penalized criteria but have only asymptotic justification. Herein, we use the key result of Birgé & Massart [1] to give the form of pen(m) and a risk bound of the penalized estimator of S (denoted by $\tilde{S}$) from a non-asymptotic point of view.

Proposition 1: There exist two postitive constants $K > 1$ and $\theta > 0$ such that if the penalty is defined for all model $m \in \mathcal{M}$ by:

$$\text{pen(m)} = K\, D_m\, \sigma^2 \Big(1 + \sqrt{\theta + \frac{2\log(card_{\mathcal{M}}(D_m))}{D_m}}\Big)^2 \quad (4)$$

then the penalized estimator $\tilde{S}$ satisfies:

$$\mathbb{E}\|S - \tilde{S}\|^2 \leq C(K) \inf_{m \in \mathcal{M}} \Big\{\|S - \bar{S}_m\|^2 + \text{pen}(m)\Big\} + C'(K, \theta)\sigma^2 \quad (5)$$

where $card_{\mathcal{M}}(D)$ represents the number of the models $m \in \mathcal{M}$ having the dimension D, and $\bar{S}_m$ is the projection of S on m ■

Proof. Using the following result of Birgé & Massart [1]:

Theorem 1 (Birgé and Massart): Let's consider the Gaussian framework (1) and let define a familiy of non-negative weights $\{L_{m \in \mathcal{M}}\}$ satisfying:

$$\Sigma = \sum_{m \in \mathcal{M} | D_m > 0} e^{-L_m D_m} < \infty. \quad (6)$$

Let's now consider a penalty function pen$(.)$ satisfying:

$$\text{pen}(m) \geq K\sigma^2 D_m (1 + \sqrt{2L_m})^2 \quad (7)$$

for all $m \in \mathcal{M}$ and some $K > 1$, then the penalized estimator $\tilde{S}$ exists almost surely and is unique. Moreover, it satisfies the following inequation:

$$\mathbb{E}\|S - \tilde{S}\|^2 \leq C(K) \inf_{m \in \mathcal{M}} \Big\{\|S - \bar{S}_m\|^2 + \text{pen}(m)\Big\} + C'(K)\Sigma\sigma^2 \quad (8)$$

■

then, it amounts to find the (optimal) weights $\{L_{m \in \mathcal{M}}\}$. We have:

$$\begin{aligned} \Sigma &= \sum_{m \in \mathcal{M}} e^{-L_m D_M} = \sum_{D=D_{min}}^{D_{max}} e^{-L_D\, D} card_{\mathcal{M}}(D) \\ &= \sum_{D=D_{min}}^{Dmax} e^{-D(L_D - \frac{\log card_{\mathcal{M}}(D)}{D})} \end{aligned}$$

Let put: $L_m = L_{D_m} = \theta + \frac{\log card_{\mathcal{M}}(D_m)}{D_m}$, for some $\theta > 0$, then we get:

$$\Sigma = \Sigma(\theta) = \sum_{D=D_{min}}^{D_{max}} e^{-D\theta} = \frac{e^{-D_{min}\theta} - e^{-(D_{max}+1)\theta}}{1 - e^{-\theta}}$$

We replace $\{L_{m \in \mathcal{M}}\}$ in (7) and $\Sigma(\theta)$ in (8), to establish the proof of the proposition 1 ■

Remark. In contrast to Lebarbier [9] who applied a similar result for the problem of change detection in the mean of $1D$ Gaussian process and who used only a rough formula for pen(m), in this paper, we use dynamic programming to compute exactly $card_{\mathcal{M}}(D)$ hence pen(m). This results in a lower risk bound of the penalized estimator $\tilde{S}$.

3) Computing $\tilde{S}$: Minimizing (3) on $\mathscr{S}$ is quite an NP-hard problem. So, instead of minimizing (3) on $\mathscr{S}$, our idea is to minimize it only on a subset of $\mathscr{S}$ that we think contains good candidate estimators of S. We construct such condidate estimators as follows: First, we consider a time partition $\mathcal{T}$. For each time interval τ of $\mathcal{T}$, we compute the mean intensity value for each signal of the packet of signals, and we order these mean values in a descending order. Indeed, it is natural to put together the signal segments with higher mean intensity values and together those with lower mean intensity values. Thus, the decision in each time interval τ of $\mathcal{T}$ on the signal index where to cut the signals' mean values into one or two sets yields a spatio-temporal partition. The set of all such spatio-temporal partitions is denoted by $\mathcal{M}^*$ and the associated set of estimators is denoted by $\mathscr{S}^*$. The algorithm we present herein uses dynamic programming

to compute $card_{\mathcal{M}*}(D)$ and finds the best estimator of S for a given dimension $D, D_{min} \leq D \leq D_{max}$. We denote it by $\hat{S}_D$. $\hat{S}_D$ minimizes the sum of square differences to data among all the estimators of the class $\mathscr{S}^*$ having the dimension D. Denote by: $\gamma(P)$ the cost ($\mathcal{L}^2$ distance to data) of a time-space part $P = \tau \times I$ after the ordering operation of the mean intensity values with respect to the time interval τ as we explained it earlier in this subsection, w and W are respectively the minimal and the maximal temporal lengths of a time-space part, h is the minimal spatial length (minimal number of signal indexes) of a time-space part [2]. We define $\hat{\Delta}_{t,D}$ and $C_{t,D}$ respectively as the cost of the minimal estimator and the cardinal of the set of the estimators of class $\mathscr{S}^*$ of the part of data $\{y_i(s), i = 1 \ldots, M, s = t, \ldots, N\}$ having the dimension D. Then, we seek to compute $\hat{\Delta}_{1,D}$ (*ie.* the cost of $\hat{S}_D$) and $C_{1,D}$ (*ie.* $card_{\mathcal{M}*}(D)$), for $D = D_{min}, \ldots, D_{max}$. The following general recursive formulas allow their calculation, and because of lack of space, the dear reader must handle the initialization step (border terms).

$$\hat{\Delta}_{t,D} = \min_{\substack{min(N-w,t+W-1)\geq u\geq t+w \\ h\leq i\leq M-1}} \Big\{\gamma_{t,u,1,i} + \gamma_{t,u,i+1,M} + \hat{\Delta}_{u+1,D-2}, \gamma_{t,u,1,M} + \hat{\Delta}_{u+1,D-1}\Big\}, N - W + 1 \leq t \leq N - w + 1, D_{min} \leq D \leq D_{max}$$

$$C_{t,D} = \sum_{\substack{min(N-w+1,t+W-1)\geq u\geq t+w \\ N-W+1\leq t\leq N-w+1, D_{min}\leq D\leq D_{max}}} C_{u,D-1} + (M-h) \times C_{u,D-2}$$

Once one has computed $\hat{S}_D$ and $card_{\mathcal{M}^*}(D)$ for $D = D_{min}, \ldots, D_{max}$, (3) is minimized on D to find $\tilde{S}$.

4) Method calibration: K and θ are trade-off parameters in (5). As their optimal values depend on the unknown S, we adjusted them by simulation. It turns out that $K = 2$ and $\theta = 2$ behave some like universal constants. For σ which is assumed to be known so far, we propose a fast and simple method for its estimation. As we assumed that the variance of the 2D signal y is the same as the variance of each of the 1D signals $y_i, i = 1, \ldots, M$, so, let's first estimate the variance σ_i^2 of y_i. Define $z_i(t) = y_i(t + 1) - y_i(t), t = 1, \ldots, N - 1$. Let's now consider $z_i^*(t) = z_i(2t - 1), t = 1, \ldots, [\frac{N+1}{2}]$ and $z_i^{**}(t) = z_i(2t), t = 1, \ldots, [\frac{N}{2}]$. If there was no significant fluorescence change in the signal y_i, then both $z_i^*(t), t = 1, \ldots, [\frac{N+1}{2}]$, and $z_i^{**}(t), t = 1, \ldots, [\frac{N}{2}]$ would be *i.i.d* Gaussians with variance $2\sigma_i^2$. In presence of significant fluorescence change due to vesicle trafficking, both $z_i^*(t), t = 1, \ldots, [\frac{N+1}{2}]$ and $z_i^{**}(t), t = 1, \ldots, [\frac{N}{2}]$ may be viewed as *i.i.d* Gaussians with variance $2\sigma_i^2$ but contain outliers. Thus, a robust estimator of $2\sigma_i^2$ is needed. A good robust estimator of the standard deviation s of Gaussian process $\epsilon_t, t = 1, \ldots, K$ is: $\hat{s} = 1.5 \times Median(|\epsilon_t|, t = 1, \ldots, K)$. So, two estimators of $\sqrt{2}\sigma_i$ are: $\hat{s}_1 = 1.5 \times Median\{|z_i^*(t)|, t = 1, \ldots, [\frac{N+1}{2}]\}$ and $\hat{s}_2 = 1.5 \times Median\{|z_i^{**}(t)|, t = 1, \ldots, [\frac{N}{2}]\}$. It follows that an estimator of σ_i is: $\hat{\sigma}_i = \frac{\hat{s}_1 + \hat{s}_2}{2\sqrt{2}}$, and finally an estimator of σ is: $\hat{\sigma} = Median\{\hat{\sigma}_i, i = 1, \ldots, M\}$.

[2] w, W and h are by default respectively equal to 1 ,N , and 1, but may also be set accordingly to trade off robust detections and fast calculations.

III. Experimental results

We used the developed approach to analyse videomicroscopic sequences of the RAB6A related vesicle trafficking. These sequences of size $395 \times 345 \times 10$ voxels$^3 \times 120$ seconds were acquired using the wide-field modality and are coded in short (intensity values range from a few tens to a few thousands).

A. Detection of activity regions

First, we divided the 3D volume into blocks (sites) of size $3 \times 3 \times 3$ and we treat at once $N = 60$ instants. For each pixel x of a site, we consider the corresponding signal y_x. To decide whether or not there is vesicle trafficking at some site X, we use *a contrario* hypothesis testing Desolneux et *al.*, 2000). For each pixel x of X, we consider the null hypothesis $H_0(x)$: "No trafficking exists at pixel x" and the alternative hypothesis $H_1(x)$ "There is trafficking at pixel x". Noise is assumed to be Gaussian, so let's consider the statistic $T_x = \frac{\sum_{t=1}^{N}(y_x(t)-\bar{y}_x)^2}{\sigma_x^2}$, where $\bar{y}_x = \frac{1}{N}\sum_{t=1}^{N} y_x(t)$ and σ_x^2 is the signal variance. Notice that the statistic T_x increases as there is significant changes in the fluorescence profile y_x of the pixel x. Under $H_0(x)$, T follows a χ^2 distribution with degree of freedom $N - 1$. So, we fix a *p*-value α (*eg.* $\alpha = 5\%$), and we determine the quantile A_x such that $\mathbf{P}(T_x \geq A_x / H_0(x)) = \alpha$. Finally, we decide to select the site X if $T_x \geq A_x$ for at least six pixels x of X. For instance, for the sequence shown in Fig1.a, around 15.900 image sites (*cf.* Fig2.a) were detected ($\alpha = 5\%$).

B. Trafficking Analysis & quantification

The described approach is applied on the so detected sites. For instance, for the packet of signals of Fig1.b, the program was run with the parameters $w = 2, W = 60$, and $h = 6$, and the found penalized estimator (for visualization convenience, the optimal ordering found by the algorithm is considered) is shown in Fig2.b. An other example of multiple vesicle passages with heavy background is presented in Fig2.c and Fig2.d. Since the minimum number of averaged observations in each spatio-temporal part of the optimal spatio-temporal partition is $w \times h$ (*ie*. 12 here), the estimation of the mean in each of the spatio-temporal partitions is robust to noise and approaches well the average fluorescence of either the background or the vesicles. Thus, vesicle trafficking can be viewed as significant change in the fluorescence of a site in the image during a few time instants. So, we consider the $1D$ function F obtained from $\tilde{S}$ by considering the successive larger values of each time interval of the optimal spatio-temporal partition as shown in Fig2.e. Vesicle trafficking at a site corresponds then to the hills and the background to the valleys of F. If one knows the average fluorescence of the objects of interest in the image (vesicles), a simple thresholding of F suffices to make the separation "moving object *vs* background". However, in absence of this information, an adapted thresholding is needed. One possibility is the $1D$ watershed transform applied to F (up to some post-processing to handle insignificant changes). From this analysis, we can envisage many applications that lead the user

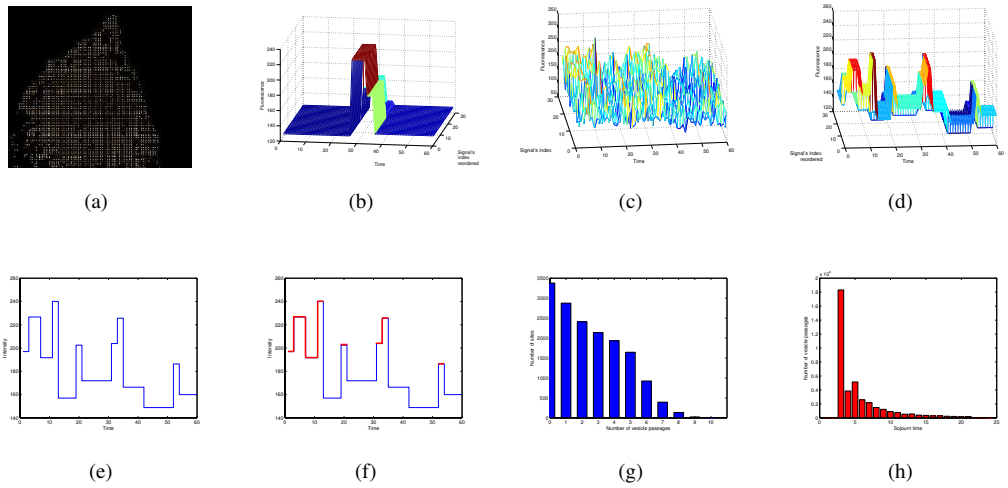

(a) (b) (c) (d)

(e) (f) (g) (h)

Fig. 2. *(a) A 2D slice of the 3D binary image of the detected trafficking sites (in white) ($\alpha = 5\%$) ; (b) A 3D representation of the observed trafficking (penalized estimator (up to a reordering)) for the signal packet of Fig1.b ($w = 2, W = 60, h = 6$) ; The algorithm found that $\tilde{S} = \hat{S}_6$ (colour is for visualization convenience only) ; (c) A packet of the 27 signals of a site X ; (b) The corresponding penalized estimator (up to a reordering) ($w = 2, W = 10, h = 6$) ; (e) Constructing the $1D$ function F ; (f) Detection by simple thresholding of vesicle trafficking at the site X (here a threshold of 180 is used). As shown in the figure, four vesicle passages are detected (coloured in red); (g) The histogram of trafficking frequency ; (h) The histogram of sojourn times of vesicles at the detected image sites.*

in his understanding of the dynamics in the scene. Indeed, depending on the aspects of the sequence dynamics the user wants to study, many statistics can be computed accordingly. For instance, the two histograms shown in Fig2.g and Fig2.h respectively were obtained (using the described method) from a sequence of the RAB6A related vesicle trafficking. The first (Fig2.g) tells us the trafficking frequency *ie.* which sites are most or least visited. The second histogram (Fig2.h) summarizes the dynamics of the sequence and can be used to infer particular sites (*eg.* acceleration regions) or compare the dynamics of two cultures (*eg.* healthy *vs* diseased cells), etc... So far, because of the difficulty to know the ground truth in 4D videmocicroscopy, the results were validated by superposing the detections and the original sequence, next using a volume rendering technique to appreciate visually the results. But we plan in the very near future to construct a realistic simulator of cell trafficking to assess objectively the system's performance.

IV. Conclusion & perspectives

We presented an automatic approach for spatio-temporal analysis of vesicle trafficking in 4D videomicroscopy. It constitutes an interesting framework for summarizing the huge spatio-temporal data and performing statistical analysis of dynamics in 4D videomicroscopy. On top of our efforts to improving theoretically the method's performance, we are constructing high level representations of vesicle dynamics based on the described approach and on graph theory. This aims at developping a GUI (Graphical User Interface) that allows the user to navigate intelligently in the spatio-temporal content of the sequence, focus on special sites, select special dynamics, visualize particular scenes of the sequence, add missing information, etc ....

V. Acknowledgments

The authors would like to thank V. Racine, J. Salamero, and J.B. Sibarita of the team *Compartments and cell dynamics - UMR 144 CNRS/Curie Institute of Paris*, for providing us with the 4D raw and deconvoluted videomicroscopic sequences we used in this work, and Mrs. S. Huet for her valuable remarks and suggestions.

References

[1] Birgé, L. and Massart, P. Gaussian Model Selection. *J. European Math. Soc.3*, pp.203-268, 2001.

[2] Bonneau, S. ; Dahan, M. and Cohen, L.D. Single Quantum Dot Tracking Based on Perceptual Grouping Using Minimal Paths in a Spatiotemporal Volume. *IEEE Trans. Imag. Proc.* 14(9), pp. 1384-1395, 2005.

[3] Boulanger, J. ; Kervrann, C. and Bouthemy, P. An adaptive statistical method for 4D fluorescence image sequences denoising with spatio-temporal discontinuities preserving. *Proc. Int. Conf. Image Processing (ICIP'05)*, Genova, Italy, 2005.

[4] Boulanger, J. ; Kervrann, C. ; Bouthemy, P. Estimation of dynamic background for fluorescence video-microscopy. *In Proc. Int. Conf. Image Processing (ICIP'06)*, Atlanta, USA, 2006.

[5] Chalfie, M. Tu. ; Euskirchen et *al.* Green Fluorescent protein as a marker for gene expression. *Science 263*, pp.802-805, 1994.

[6] Desolneux, A. ; Moisan, L. and Morel, J.M. Meaningful Alignements, *International Journal of Computer Vision*, Vol.40(1), pp.7-23, 2000.

[7] Genovesio, A. ; Belhassine, Z.; Olivo-Marin, J-C. Adaptive Gating in Gaussian bayesian Multi-Target Tracking. *Int. Conf. Image Processing (ICIP'04), Vol.1, pp.147-150*, Singapore, 2004.

[8] Ponti A. ; Vallotton, P. ; Salmon, E. ; Waterman-Storer, C. and Danuser, G. Computational analysis of f-actin turnover in cortical actin meshworks using fluorescent speckle microscopy. *Biophys. J.*, vol. 85, pp. 3366-3352, 2003.

[9] Lebarbier, E. Detecting multiple change-points in the mean of Gaussian process by model selection. *Signal Processing 85*, pp.717-736, 2005.

[10] Meijering, E. ; Smal, I. and Danuser, G. Tracking in molecular bioimaging. *IEEE Sig. Proc. Magaz.,* vol. 23, no. 3, pp. 46-53, 2006.

[11] Miura, K. Tracking Movement in Cell Biology. *Advances in Biochemical Engineering/Biotechnology, Vol.95*, p267 Springer Verlag, 2005.

[12] Sibarita, J.B. ; Racine, V. and Salamero, J. Quantification of membrane trafficking on a 3D cytoskeleton network in living cells, *In Proc. Int. Symp. on Biomedical Imaging (ISBI'06)*, Arlington, USA, 2006.